A trimeric tri-Tb^{3+}-including antimonotungstate and its $Eu^{3+}/Tb^{3+}/Dy^{3+}/Gd^{3+}$ codoped species with luminescence properties

Xin Xu,[a] Changtong Lu,[a,b] Saisai Xie,[a] Lijuan Chen,[a,*] and Junwei Zhao [a,*]

[a] *Henan Key Laboratory of Polyoxometalate Chemistry, College of Chemistry and Chemical Engineering, Henan University, Kaifeng, Henan 475004, China. E-mail: ljchen@henu.edu.cn, zhaojunwei@henu.edu.cn.*

[b] *China Tobacco Henan Industrial Company Ltd., Zhengzhou, Henan 475000, China.*

Electronic supplementary information

Materials and physical measurements
X-ray crystallography
Synthesis

Fig. S1. (a) IR spectrum of $\mathbf{Tb_3W_{28}}$; (b IR spectra of $\mathbf{Tb_{1.8}Eu_{3y}Gd_{1.2-3y}W_{28}}$ (y = 0.00, 0.10, 0.14, 0.18, 0.22, 0.26). (c) IR spectra of $\mathbf{Dy_{1.2}Tb_{3z}Eu_{0.03}Gd_{1.77-3z}W_{28}}$ (z = 0.00, 0.10, 0.20, 0.30, 0.40).
Fig. S2. (a) Experimental and simulative PXRD patterns of $\mathbf{Tb_3W_{28}}$; (b) Experimental PXRD patterns of $\mathbf{Tb_{1.8}Eu_{3y}Gd_{1.2-3y}W_{28}}$ (y = 0.00, 0.10, 0.14, 0.18, 0.22, 0.26); (c) Experimental PXRD patterns of $\mathbf{Dy_{1.2}Tb_{3z}Eu_{0.03}Gd_{1.77-3z}W_{28}}$ (z = 0.00, 0.10, 0.20, 0.30, 0.40).
Fig. S3. A unit cell including nine Tb^{3+} ions (Z = 9).
Fig. S4. (a) Emission spectra of $\mathbf{Tb_{1.8}Eu_{3y}Gd_{1.2-3y}W_{28}}$ (y = 0.00, 0.10, 0.14, 0.18, 0.22, 0.26) obtained upon λ_{ex} = 370 nm; (b) Dependence of emission intensity of peak at 545 and 613 nm on concentration of Tb^{3+} ions upon λ_{ex} = 370 nm; (c) Decay lifetime curves of the peaks at 545 nm for $\mathbf{Tb_{1.8}Eu_{3y}Gd_{1.2-3y}W_{28}}$ (y = 0.00, 0.10, 0.14, 0.18, 0.22, 0.26) upon λ_{ex} = 389 nm; (d) Dependence of ET_2 efficiency ($Tb^{3+}\rightarrow Eu^{3+}$) on concentration of Eu^{3+} ions upon λ_{ex} = 370 nm for $\mathbf{Tb_{1.8}Eu_{3y}Gd_{1.2-3y}W_{28}}$.
Fig. S5. Dependence of I_{S0}/I_0 of the $^5D_4\rightarrow{}^7F_5$ transition from Tb^{3+} ions on $C^{6/3}$, $C^{8/3}$ and $C^{10/3}$.
Fig. S6. (a) Decay lifetime curves of the peaks at 572 nm for $\mathbf{Dy_{1.2}Tb_{3z}Eu_{0.03}Gd_{1.77-3z}W_{28}}$ (z = 0.00, 0.10, 0.20, 0.30, 0.40) upon λ_{ex} = 389 nm; (b) Decay lifetime curves of the peaks at 613 nm for $\mathbf{Dy_{1.2}Tb_{3z}Eu_{0.03}Gd_{1.77-3z}W_{28}}$ (z = 0.00, 0.10, 0.20, 0.30, 0.40) upon λ_{ex} = 389 nm.
Fig. S7. (a) The CIE 1931 diagram of $\mathbf{Dy_{1.2}Tb_{3z}Eu_{0.03}Gd_{1.77-3z}W_{28}}$ upon various excitation (360–400 nm); (b) The CIE 1931 diagram of $\mathbf{Dy_{1.2}Tb_{3z}Eu_{0.03}Gd_{1.77-3z}W_{28}}$ upon various excitation (360–400 nm); (c) The CIE 1931 diagram of $\mathbf{Dy_{1.2}Tb_{3z}Eu_{0.03}Gd_{1.77-3z}W_{28}}$ upon various excitation (360–400 nm).
Fig. S8. (a–d) The CIE 1931 diagram of $\mathbf{Dy_{1.2}Tb_{3z}Eu_{0.03}Gd_{1.77-3z}W_{28}}$ (z = 0.00, 0.10, 0.20, 0.30, 0.40) upon various excitation (360–400 nm).
Fig. S9. TG curve of $\mathbf{Tb_3W_{28}}$.
Table S1a. The qualities and moles of $Dy(NO_3)_3{\cdot}6H_2O$, $Tb(NO_3)_3{\cdot}6H_2O$ and $Gd(NO_3)_3{\cdot}6H_2O$ for the preparations of $\mathbf{Dy_{1.2}Tb_{3x}Gd_{1.8-3x}W_{28}}$ (x = 0.00, 0.10, 0.20, 0.30, 0.40, 0.50).
Table S1b. The qualities and moles of $Tb(NO_3)_3{\cdot}6H_2O$, $Eu(NO_3)_3{\cdot}6H_2O$ and $Gd(NO_3)_3{\cdot}6H_2O$ for the preparations of $\mathbf{Tb_{1.8}Eu_{3y}Gd_{1.2-3y}W_{28}}$ (y = 0.0, 0.10, 0.14, 0.18, 0.22, 0.26).
Table S1c. The qualities and moles of $Dy(NO_3)_3{\cdot}6H_2O$, $Tb(NO_3)_3{\cdot}6H_2O$ and $Eu(NO_3)_3{\cdot}6H_2O$ for the

preparations of $\mathbf{Dy_{1.2}Tb_{3z}Eu_{0.03}Gd_{1.77-3z}W_{28}}$ (z = 0.00, 0.10, 0.20, 0.30, 0.40).

Table S1d. The analytic and experimental molar concentration of Dy^{3+}, Tb^{3+} and Gd^{3+} ions in $\mathbf{Dy_{1.2}Tb_{3x}Gd_{1.8-3x}W_{28}}$ (x = 0.00, 0.10, 0.20, 0.30, 0.40, 0.50) measured by ICP–AES spectrometer.

Table S1e. The analytic and experimental molar concentration of Tb^{3+} Eu^{3+} and Gd^{3+} ions in $\mathbf{Tb_{1.8}Eu_{3y}Gd_{1.2-3y}W_{28}}$ (y = 0.0, 0.10, 0.14, 0.18, 0.22, 0.26) measured by ICP–AES spectrometer.

Table S1f. The analytic and experimental molar concentration of Dy^{3+}, Tb^{3+} Eu^{3+} and Gd^{3+} ions in $\mathbf{Dy_{1.2}Tb_{3z}Eu_{0.03}Gd_{1.77-3z}W_{28}}$ (z = 0.00, 0.10, 0.20, 0.30, 0.40) measured by ICP–AES spectrometer.

Table S2. X-ray diffraction crystallographic data and structure refinements for $\mathbf{Tb_3W_{28}}$.

Table S3. BVS calculations of all the Tb, Sb, W and O atoms in $\mathbf{Tb_3W_{28}}$.

Table S4. Bond lengths of Tb-O bonds and bond angles of O-Tb-O bonds in $\mathbf{Tb_3W_{28}}$.

Table S5. Summary of PL lifetimes and pre-exponential factors of $\mathbf{Dy_{1.2}Tb_{3x}Gd_{1.8-3x}W_{28}}$ (x = 0.00, 0.10, 0.20, 0.30, 0.40, 0.50) by monitoring the emissions at 572 nm ($^4F_{9/2}\rightarrow{}^6H_{13/2}$) and under the excitation at 389 nm ($^6H_{15/2}\rightarrow{}^6I_{13/2}$).

Table S6. Summary of PL lifetimes and pre-exponential factors of $\mathbf{Tb_{1.8}Eu_{3y}Gd_{1.2-3y}W_{28}}$ (y = 0.0, 0.10, 0.14, 0.18, 0.22, 0.26) by monitoring the emissions at 545 nm ($^5D_4\rightarrow{}^7F_5$) and under the excitation at 370 nm ($^7F_6\rightarrow{}^5L_{10}$).

Table S7. Summary of PL lifetimes and pre-exponential factors of $\mathbf{Dy_{1.2}Tb_{3z}Eu_{0.03}Gd_{1.77-3z}W_{28}}$ (z = 0.00, 0.10, 0.20, 0.30, 0.40) by monitoring the emissions at 572 nm ($^4F_{9/2}\rightarrow{}^6H_{13/2}$) and under the excitation at 389 nm ($^6H_{15/2}\rightarrow{}^6I_{13/2}$).

Table S8. Summary of PL lifetimes and pre-exponential factors of $\mathbf{Dy_{1.2}Tb_{3z}Eu_{0.03}Gd_{1.77-3z}W_{28}}$ (z = 0.00, 0.10, 0.20, 0.30, 0.40) by monitoring the emissions at 613 nm ($^5D_0\rightarrow{}^7F_2$) and under the excitation at 389 nm ($^6H_{15/2}\rightarrow{}^6I_{13/2}$).

Table S9. Comparison of optical parameters for $\mathbf{Dy_{1.2}Tb_{0.3}Eu_{0.03}Gd_{1.47}W_{28}}$ under different excitation wavelengths.

Table S10. Comparison of optical parameters for $\mathbf{Dy_{1.2}Tb_{0.6}Eu_{0.03}Gd_{1.17}W_{28}}$ under different excitation wavelengths.

Table S11. Comparison of optical parameters for $\mathbf{Dy_{1.2}Tb_{0.9}Eu_{0.03}Gd_{0.87}W_{28}}$ under different excitation wavelengths.

Table S12. Comparison of optical parameters for $\mathbf{Dy_{1.2}Tb_{1.2}Eu_{0.03}Gd_{0.57}W_{28}}$ under different excitation wavelengths.

Materials and physical measurements

$Na_9[B\text{-}\alpha\text{-}SbW_9O_{33}]\cdot 19.5H_2O$ was prepared according to the reported method.[1] All reagents were purchased directly without further purification. The contents of C and H elements were measured on a Vario EL Cube CHNS analyzer. The contents of Na, W, Sb, Tb, Gd, Eu, Dy elements were measured by inductively coupled plasma atomic emission spectrometry (ICP–AES) on a Perkin–Elmer Optima 2000 ICP–AES spectrometer. IR spectra were collected on Perkin–Elmer FT–IR spectrometer in the range of 400–4000 cm^{-1}. A Bruker D8 ADVANCE apparatus with Cu Kα radiation (λ = 1.54056 Å) at 293 K gave birth to the experimental PXRD patterns. TG analysis was measured on a Bruker Tensor−II TGA instrument under the N_2 atmosphere with a heating rate of 10 $^oC\ min^{-1}$ in the range of 25−1000 ^oC. Photoluminescence emission and excitation spectra were measured on a FLS 980 Edinburgh Analytical Instrument under a 450 W xenon lamp. Decay curves were obtained under the excitation of a μF900H high−energy microsecond flash lamp.

X-ray crystallography

A good-quality single-crystal of **Tb_3W_{28}** was scanned on a Bruker Apex II diffractometer equipped with CCD two−dimensional detector by using monochromated Mo Kα radiation (λ = 0.71073 Å) at 296(2) K. Through using the program SADABS, the multi-scan absorption corrections and routine Lorentz polarization were triumphantly acquired. Direct methods were used to solve its structure and located the heavy atoms using the SHELXTL–97 program package.[2–3] The remaining atoms were found from successive full-matrix least-squares refinements on F^2 and Fourier syntheses. All non-hydrogen atoms were refined anisotropically except for some water molecules. There are still solvent accessible voids in their check cif reports, which suggest that some solvent water molecules or counter cations should exist in the structure that can't be found from the weak residual electron peaks. These solvent molecules are highly disordered, and attempts to locate and refine them were unsuccessful. Based on elemental analysis and TG analysis, eleven lattice water molecules and eight Na^+ cations were directly added to the molecular formula. Crystallographic data of **Tb_3W_{28}** are put in Table S2. Its cif file was deposited at the Cambridge Crystallographic Data Centre with CCDC 2007609 and can be freely downloaded on www.ccdc.cam.ac.uk/data_request/cif. from the Cambridge Crystallographic Data Centre.

Synthesis of $Na_{17}\{(WO_4)[Tb(H_2O)(Ac)(B\text{-}\alpha\text{-}SbW_9O_{31}(OH)_2)]_3\}\cdot 50H_2O$ (Tb_3W_{28})

The solid-state $Na_9[B\text{-}\alpha\text{-}SbW_9O_{33}]\cdot 19.5H_2O$ (3.500 g, 1.222 mmol) and $Na_2WO_4\cdot 2H_2O$ (0.200 g, 0.607 mmol) were dissolved in 15 mL of NaAc/HAc buffer solution (2 mol/L, pH = 5.50) upon stirring. Whereafter, $Tb(NO_3)_3\cdot 6H_2O$ (0.400 g, 0.883 mmol) was added upon stirring. The pH value of the mixture was adjusted to 5.50 again by using HCl (6 mol/L) and the mixture was stirred for 30 min. The mixture was kept in the 90 °C water bath for 1 h. After being taken out, it was cooled to room temperature and filtered. Slow evaporation of the filtrate at room temperature led to laurel-green hexagonal crystals of **Tb_3W_{28}** for about three days. Yield: 1.01 g (37.4%) (based on $Tb(NO_3)_3\cdot 6H_2O$). Elemental analysis (%) calcd: C, 0.77; H, 1.36; Na, 5.63; W, 54.85; Sb, 3.89; Tb, 4.86. Found: C, 0.91; H, 1.17; Na, 5.45; W, 55.09; Sb, 3.71; Tb, 5.03. IR (KBr, cm^{-1}): 3346(vs), 1632(s), 1531 (s), 1462(s), 935(m), 887(w), 788(vs), 686(m).

Syntheses of $Dy_{1.2}Tb_{3x}Gd_{1.8-3x}W_{28}$, $Tb_{1.8}Eu_{3y}Gd_{1.2-3y}W_{28}$ and $Dy_{1.2}Tb_{3z}Eu_{0.03}$-$Gd_{1.77-3z}W_{28}$

The syntheses of **$Dy_{1.2}Tb_{3x}Gd_{1.8-3x}W_{28}$** ($x$ = 0.00, 0.10, 0.20, 0.30, 0.40, 0.50), **$Tb_{1.8}Eu_{3y}Gd_{1.2-3y}W_{28}$** ($y$ = 0.00, 0.10, 0.14, 0.18, 0.22, 0.26) and **$Dy_{1.2}Tb_{3z}Eu_{0.03}Gd_{1.77-3z}W_{28}$** ($z$ = 0.00, 0.10, 0.20, 0.30, 0.40)

materials were the same as that of **Tb_3W_{28}**, except that the $Eu(NO_3)_3{\cdot}6H_2O$, $Tb(NO_3)_3{\cdot}6H_2O$, $Gd(NO_3)_3{\cdot}6H_2O$ and $Dy(NO_3)_3{\cdot}6H_2O$ in place of $Tb(NO_3)_3{\cdot}6H_2O$ in the appropriate molar ratio (see the Electronic Supporting Information Tables S1a–S1c).

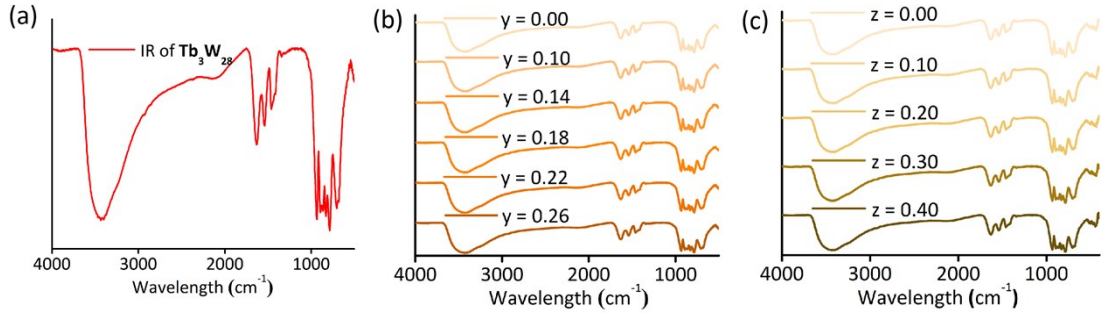

Fig. S1. (a) IR spectrum of **Tb_3W_{28}**; (b IR spectra of **$Tb_{1.8}Eu_{3y}Gd_{1.2-3y}W_{28}$** ($y$ = 0.00, 0.10, 0.14, 0.18, 0.22, 0.26). (c) IR spectra of **$Dy_{1.2}Tb_{3z}Eu_{0.03}Gd_{1.77-3z}W_{28}$** ($z$ = 0.00, 0.10, 0.20, 0.30, 0.40).

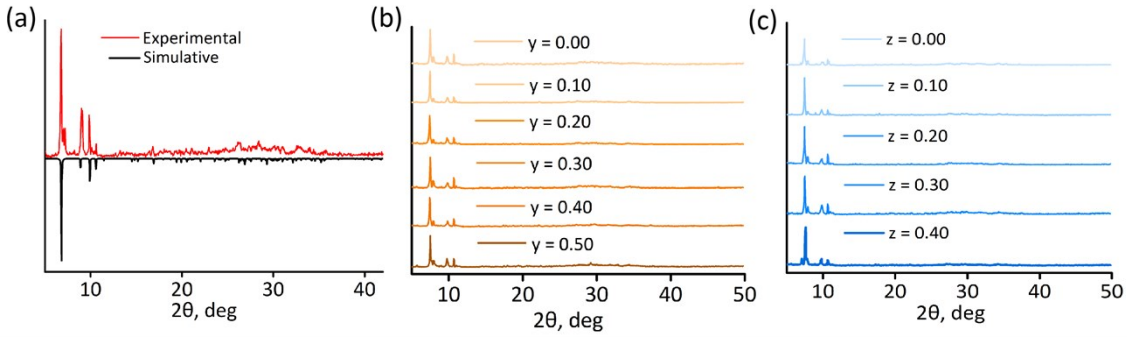

Fig. S2. (a) Experimental and simulative PXRD patterns of **Tb_3W_{28}**; (b) Experimental PXRD patterns of **$Tb_{1.8}Eu_{3y}Gd_{1.2-3y}W_{28}$** ($y$ = 0.00, 0.10, 0.14, 0.18, 0.22, 0.26); (c) Experimental PXRD patterns of **$Dy_{1.2}Tb_{3z}Eu_{0.03}Gd_{1.77-3z}W_{28}$** ($z$ = 0.00, 0.10, 0.20, 0.30, 0.40).

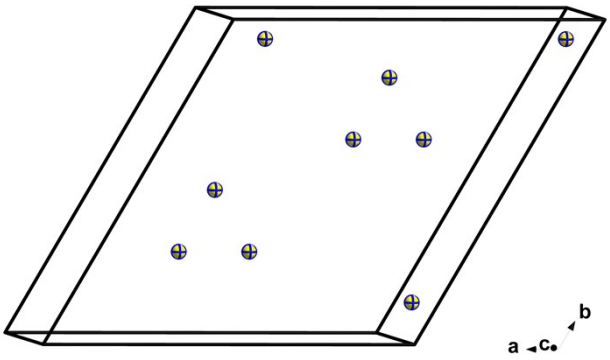

Fig. S3. A unit cell including nine Tb^{3+} ions (Z = 9).

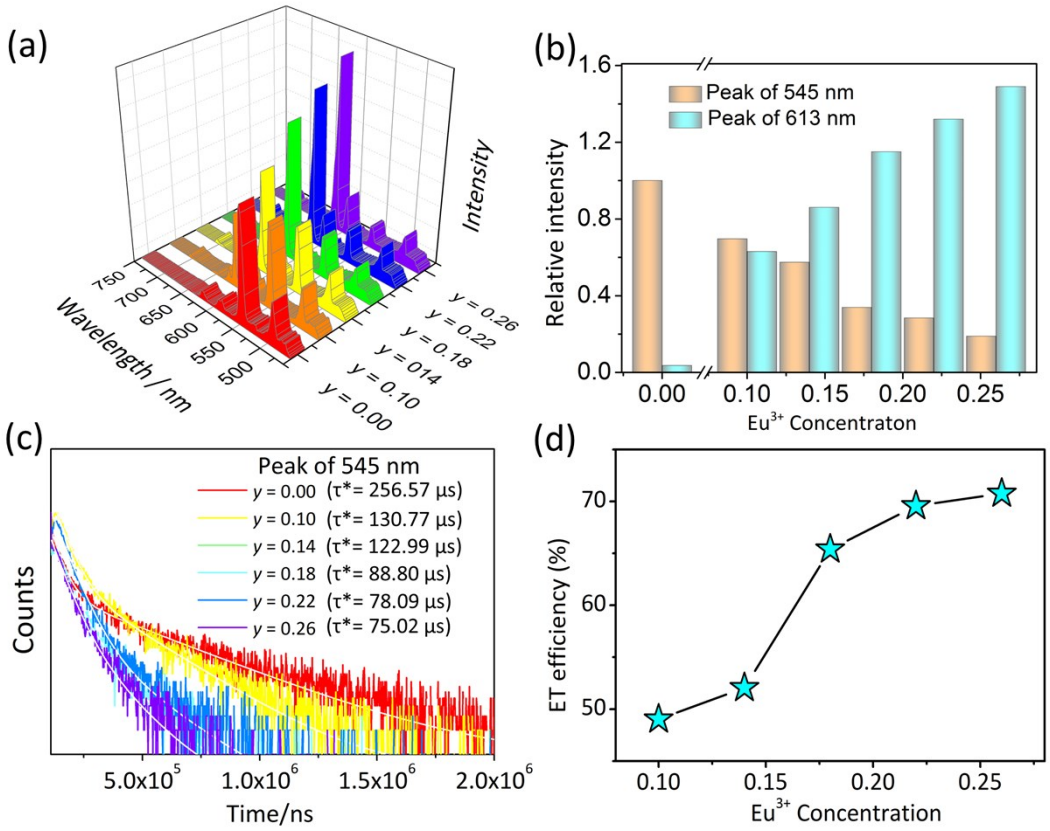

Fig. S4. (a) Emission spectra of $\mathbf{Tb_{1.8}Eu_{3y}Gd_{1.2-3y}W_{28}}$ (y = 0.00, 0.10, 0.14, 0.18, 0.22, 0.26) obtained upon λ_{ex} = 370 nm; (b) Dependence of emission intensity of peak at 545 and 613 nm on concentration of Tb^{3+} ions upon λ_{ex} = 370 nm; (c) Decay lifetime curves of the peaks at 545 nm for $\mathbf{Tb_{1.8}Eu_{3y}Gd_{1.2-3y}W_{28}}$ (y = 0.00, 0.10, 0.14, 0.18, 0.22, 0.26) upon λ_{ex} = 389 nm; (d) Dependence of ET_2 efficiency ($Tb^{3+}\rightarrow Eu^{3+}$) on concentration of Eu^{3+} ions upon λ_{ex} = 370 nm for $\mathbf{Tb_{1.8}Eu_{3y}Gd_{1.2-3y}W_{28}}$.

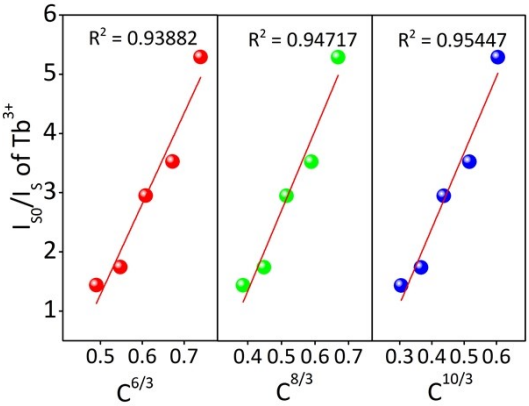

Fig. S5. Dependence of I_{S0}/I_0 of the $^5D_4\rightarrow{}^7F_5$ transition from Tb^{3+} ions on $C^{6/3}$, $C^{8/3}$ and $C^{10/3}$.

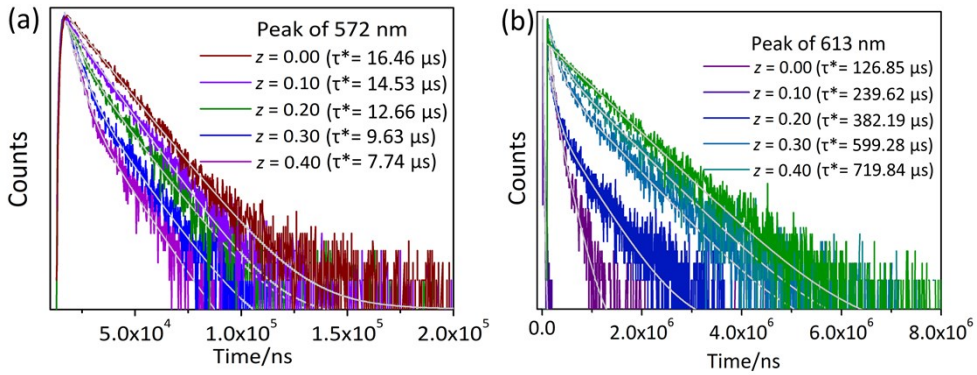

Fig. S6. (a) Decay lifetime curves of the peaks at 572 nm for $\mathbf{Dy_{1.2}Tb_{3z}Eu_{0.03}Gd_{1.77-3z}W_{28}}$ (z = 0.00, 0.10, 0.20, 0.30, 0.40) upon λ_{ex} = 389 nm; (b) Decay lifetime curves of the peaks at 613 nm for $\mathbf{Dy_{1.2}Tb_{3z}Eu_{0.03}Gd_{1.77-3z}W_{28}}$ (z = 0.00, 0.10, 0.20, 0.30, 0.40) upon λ_{ex} = 389 nm.

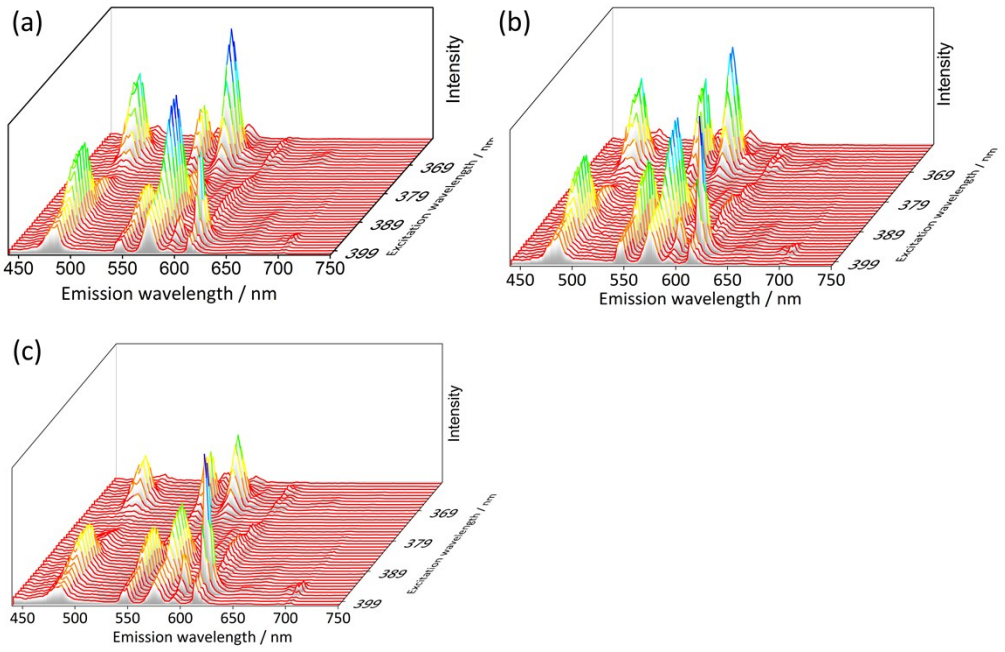

Fig. S7. (a) The CIE 1931 diagram of $\mathbf{Dy_{1.2}Tb_{3z}Eu_{0.03}Gd_{1.77-3z}W_{28}}$ upon various excitation (360–400 nm); (b) The CIE 1931 diagram of $\mathbf{Dy_{1.2}Tb_{3z}Eu_{0.03}Gd_{1.77-3z}W_{28}}$ upon various excitation (360–400 nm); (c) The CIE 1931 diagram of $\mathbf{Dy_{1.2}Tb_{3z}Eu_{0.03}Gd_{1.77-3z}W_{28}}$ upon various excitation (360–400 nm).

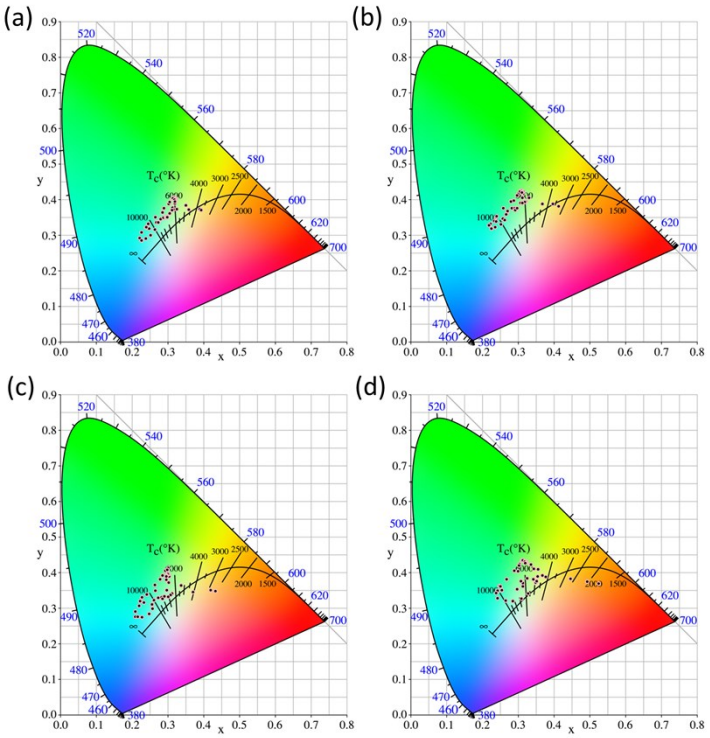

Fig. S8. (a–d) The CIE 1931 diagram of $\mathbf{Dy_{1.2}Tb_{3z}Eu_{0.03}Gd_{1.77-3z}W_{28}}$ (z = 0.00, 0.10, 0.20, 0.30, 0.40) upon various excitation (360–400 nm).

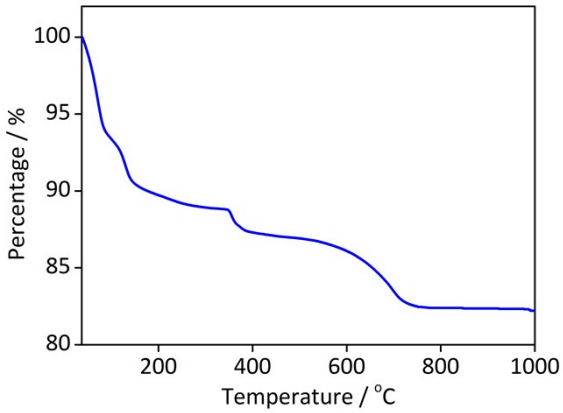

Fig. S9. TG curve of $\mathbf{Tb_3W_{28}}$.

Thermal stability

The TG measurement of $\mathbf{Tb_3W_{28}}$ was collected in flowing N_2 atmosphere from 25 to 1000 °C with a heating rate of 10 °C min^{-1} to test the thermostability (Fig. S9). The TG analysis illustrates that $\mathbf{Tb_3W_{28}}$ undergo a two-step weight loss. The first weight loss from 25 to 320 °C of 11.15 % (calcd. 10.90 %) was assigned to liberation of 50 lattice water molecules, three coordinated water molecules and the dehydration of six H^+ protons. The second weight loss from 320 to 1000 °C of 6.65 % (calcd. 7.03 %) resulted from the remove of three acetate groups and the sublimation of two WO_3 groups.

Table S1a. The qualities and moles of $Dy(NO_3)_3·6H_2O$, $Tb(NO_3)_3·6H_2O$ and $Gd(NO_3)_3·6H_2O$ for the preparations of $\mathbf{Dy_{1.2}Tb_{3x}Gd_{1.8-3x}W_{28}}$ (x = 0.00, 0.10, 0.20, 0.30, 0.40, 0.50).

x	$Dy(NO_3)_3·6H_2O$ (g)	(mmol)	$Tb(NO_3)_3·6H_2O$ (g)	(mmol)	$Gd(NO_3)_3·6H_2O$ (g)	(mmol)
0.00	0.164	0.359	0	0	0.243	0.538
0.10	0.164	0.359	0.0401	0.090	0.202	0.449
0.20	0.164	0.359	0.081	0.179	0.162	0.359
0.30	0.164	0.359	0.122	0.269	0.121	0.269
0.40	0.164	0.359	0.163	0.359	0.081	0.179
0.50	0.164	0.359	0.203	0.449	0.040	0.090

Table S1b. The qualities and moles of $Tb(NO_3)_3·6H_2O$, $Eu(NO_3)_3·6H_2O$ and $Gd(NO_3)_3·6H_2O$ for the preparations of $\mathbf{Tb_{1.8}Eu_{3y}Gd_{1.2-3y}W_{28}}$ (y = 0.0, 0.10, 0.14, 0.18, 0.22, 0.26).

y	$Tb(NO_3)_3·6H_2O$ (g)	(mmol)	$Eu(NO_3)_3·6H_2O$ (g)	(mmol)	$Gd(NO_3)_3·6H_2O$ (g)	(mmol)
0.00	0.244	0.538	0	0	0.359	0.162
0.10	0.244	0.538	0.040	0.090	0.269	0.121
0.14	0.244	0.538	0.056	0.126	0.233	0.105
0.18	0.244	0.538	0.072	0.161	0.197	0.089
0.22	0.244	0.538	0.088	0.197	0.161	0.073
0.26	0.244	0.538	0.104	0.233	0.125	0.057

Table S1c. The qualities and moles of $Dy(NO_3)_3·6H_2O$, $Tb(NO_3)_3·6H_2O$ and $Eu(NO_3)_3·6H_2O$ for the preparations of $\mathbf{Dy_{1.2}Tb_{3z}Eu_{0.03}Gd_{1.77-3z}W_{28}}$ (z = 0.00, 0.10, 0.20, 0.30, 0.40).

z	$Dy(NO_3)_3·6H_2O$ (g)	(mmol)	$Tb(NO_3)_3·6H_2O$ (g)	(mmol)	$Eu(NO_3)_3·6H_2O$ (g)	(mmol)	$Gd(NO_3)_3·6H_2O$ (g)	(mmol)
0.00	0.123	0.269	0	0	0.04	0.009	0.279	0.619
0.10	0.123	0.269	0.041	0.090	0.04	0.009	0.239	0.529
0.20	0.123	0.269	0.081	0.179	0.04	0.009	0.198	0.440
0.30	0.123	0.269	0.122	0.269	0.04	0.009	0.158	0.350
0.40	0.123	0.269	0.163	0.358	0.04	0.009	0.117	0.260

Table S1d. The analytic and experimental molar concentrations of Dy^{3+}, Tb^{3+} and Gd^{3+} ions in $\mathbf{Dy_{1.2}Tb_{3x}Gd_{1.8-3x}W_{28}}$ (x = 0.00, 0.10, 0.20, 0.30, 0.40, 0.50) measured by ICP–AES spectrometer.

x	Analysis			Found		
	Dy^{3+}	Tb^{3+}	Gd^{3+}	Dy^{3+}	Tb^{3+}	Gd^{3+}
0.00	1.94	0	3.12	2.12	0	2.97
0.10	1.94	0.49	2.60	2.09	0.45	2.41
0.20	1.94	0.97	2.08	2.06	0.94	1.84
0.30	1.94	1.46	1.56	2.01	1.63	1.28
0.40	1.95	2.08	1.04	1.97	2.17	0.83
0.50	1.95	2.60	0.52	1.95	2.62	0.32

Table S1e. The analytic and experimental molar concentrations of Tb^{3+} Eu^{3+} and Gd^{3+} ions in $\mathbf{Tb_{1.8}Eu_{3y}Gd_{1.2-3y}W_{28}}$ (y = 0.0, 0.10, 0.14, 0.18, 0.22, 0.26) measured by ICP–AES spectrometer.

y	Analysis			Found		
	Tb^{3+}	Eu^{3+}	Gd^{3+}	Eu^{3+}	Tb^{3+}	Gd^{3+}

0.00	2.92	0	1.94	3.16	0	1.70
0.10	2.92	0.49	1.46	2.80	0.61	1.35
0.14	2.92	0.68	1.26	2.89	0.80	1.17
0.18	2.92	0.87	1.07	2.91	0.99	0.96
0.22	2.92	1.07	0.87	3.26	1.00	0.70
0.26	2.92	1.26	0.68	3.21	1.20	0.55

Table S1f. The analytic and experimental molar concentrations of Dy^{3+}, Tb^{3+} Eu^{3+} and Gd^{3+} ions in $\mathbf{Dy_{1.2}Tb_{3z}Eu_{0.03}Gd_{1.77-3z}W_{28}}$ (z = 0.00, 0.10, 0.20, 0.30, 0.40) measured by ICP–AES spectrometer.

z	Analysis				Found			
	Dy^{3+}	Tb^{3+}	Eu^{3+}	Gd^{3+}	Dy^{3+}	Tb^{3+}	Eu^{3+}	Gd^{3+}
0.00	1.94	0	0.05	2.87	2.26	0	0.07	2.64
0.10	1.94	0.49	0.05	2.38	2.29	0.47	0.06	2.18
0.20	1.94	0.97	0.05	1.90	2.20	1.04	0.06	1.64
0.30	1.94	1.46	0.05	1.41	2.11	1.57	0.08	1.28
0.40	1.94	1.94	0.05	0.92	2.13	1.70	0.06	0.77

Table S2. X-ray diffraction crystallographic data and structure refinements for $\mathbf{Tb_3W_{28}}$.

	$\mathbf{Tb_3W_{28}}$
Empirical formula	$C_6H_{121}Tb_3Na_{17}O_{162}Sb_3W_{28}$
Formula weight	9166.67
Crystal system	trigonal
Space group	*R3m*
a, Å	30.8691(6)
b, Å	30.8691(6)
c, Å	14.8152(4)
α, deg	90
β, deg	90
γ, deg	120
V, $Å^{-3}$	12226.0(5)
Z	3
μ, mm^{-1}	21.599
F(000)	12180
T, K	150(2)
Limiting indices	$-36 \le h \le 36$ $-36 \le k \le 34$ $-17 \le l \le 17$
No. of reflections collected	23056
No. of independent reflections	4809
R_{int}	0.0687
Data/restrains/parameters	4809 / 19 / 307
GOF on F^2	1.081
Final *R* indices [$I > 2\sigma(I)$]	R_1 = 0.0589 wR_2 = 0.1556
R indices (all data)	R_1 = 0.0627 wR_2 = 0.0864

Table S3. BVS calculations of all the Tb, Sb, W and O atoms in **Tb_3W_{28}**.

Atom	Tb1	Sb1	W1	W2	W3	W4	W5	W6	O1	O2	O3
BVS	3.14	3.43	6.02	6.29	6.06	6.14	6.27	5.87	2.30	1.99	1.57
Atom	O4	O5	O6	O7	O8	O9	O10	O11	O12	O13	
BVS	1.20	1.85	1.70	1.92	1.87	1.78	2.10	1.92	1.75	2.02	
Atom	O14	O15	O16	O17	O18	O19	O20	O21	O22	O23	
BVS	1.77	2.02	1.76	2.01	2.06	1.79	2.01	1.73	1.63	1.63	

Table S4. Bond lengths of Tb-O bonds and bond angles of O-Tb-O bonds in **Tb_3W_{28}**.

Tb(1)-O(7)	2.28(3)	Tb(1)-O(12)#5	2.40(2)
Tb(1)-O(1W)	2.36(4)	Tb(1)-O(12)	2.40(2)
Tb(1)-O(1)#5	2.376(18)	Tb(1)-O(14)	2.42(3)
Tb(1)-O(1)	2.376(18)	Tb(1)-O(19)	2.44(3)
O(7)-Tb(1)-O(1W)	71(2)	O(12)#5-Tb(1)-O(12)	71.1(9)
O(7)-Tb(1)-O(1)#5	95.6(5)	O(7)-Tb(1)-O(14)	154.9(14)
O(1W)-Tb(1)-O(1)#5	77.5(6)	O(1W)-Tb(1)-O(14)	134(2)
O(7)-Tb(1)-O(1)	95.6(5)	O(1)#5-Tb(1)-O(14)	91.3(5)
O(1W)-Tb(1)-O(1)	77.5(6)	O(1)-Tb(1)-O(14)	91.3(5)
O(1)#5-Tb(1)-O(1)	147.4(10)	O(12)#5-Tb(1)-O(14)	82.1(8)
O(7)-Tb(1)-O(12)#5	77.5(10)	O(12)-Tb(1)-O(14)	82.1(8)
O(1W)-Tb(1)-O(12)#5	132.0(13)	O(7)-Tb(1)-O(19)	152.5(14)
O(1)#5-Tb(1)-O(12)#5	70.7(7)	O(1W)-Tb(1)-O(19)	82(2)
O(1)-Tb(1)-O(12)#5	141.8(6)	O(1)#5-Tb(1)-O(19)	78.0(5)
O(7)-Tb(1)-O(12)	77.5(10)	O(1)-Tb(1)-O(19)	78.0(5)
O(1W)-Tb(1)-O(12)	132.0(13)	O(12)#5-Tb(1)-O(19)	123.6(7)
O(1)#5-Tb(1)-O(12)	141.8(6)	O(12)-Tb(1)-O(19)	123.6(7)
O(1)-Tb(1)-O(12)	70.7(7)	O(14)-Tb(1)-O(19)	52.6(11)

Table S5. Summary of PL lifetimes and pre-exponential factors of **$Dy_{1.2}Tb_{3x}Gd_{1.8-3x}W_{28}$** ($x$ = 0.00, 0.10, 0.20, 0.30, 0.40, 0.50) by monitoring the emissions at 572 nm ($^4F_{9/2}\rightarrow{}^6H_{13/2}$) and under the excitation at 389 nm ($^6H_{15/2}\rightarrow{}^6I_{13/2}$). [$\tau^* = (A_1\tau_1^2+A_2\tau_2^2)/(A_1\tau_1+A_2\tau_2)$][1]

x	λ_{ex} (nm)	λ_{em} (nm)	τ_1 (μs)	A_1	Percentage (%)	τ_2 (μs)	A_2	Percentage (%)	χ^2	τ^*
0.0	389	572	9.75	577.42	23.86	34.27	523.95	76.14	1.092	28.42
0.1	389	572	8.94	741.17	40.08	34.53	286.94	59.92	1.031	24.27
0.2	389	572	7.34	585.18	29.32	31.11	332.54	70.68	0.953	24.14
0.3	389	572	8.26	597.26	26.54	28.54	478.38	73.46	0.978	23.16
0.4	389	572	8.61	512.34	25.37	27.82	466.60	74.63	1.023	22.92
0.5	389	572	8.29	525.84	29.25	25.66	410.85	70.75	1.037	20.58

Table S6. Summary of PL lifetimes and pre-exponential factors of **$Tb_{1.8}Eu_{3y}Gd_{1.2-3y}W_{28}$** ($y$ = 0.0,

0.10, 0.14, 0.18, 0.22, 0.26) by monitoring the emissions at 545 nm ($^5D_4 \rightarrow {}^7F_5$) and under the excitation at 370 nm ($^7F_6 \rightarrow {}^5L_{10}$).

y	λ_{ex} (nm)	λ_{em} (nm)	τ_1 (μs)	A_1	Percentage (%)	τ_2 (μs)	A_2	Percentage (%)	χ^2	τ^*
0.00	370	545	41.64	513.74	35.88	376.84	101.44	64.12	1.023	256.57
0.10	370	545	50.64	942.24	21.98	238.15	149.52	11.61	1.023	130.77
0.14	370	545	24.84	268.80	46.78	210.74	36.04	53.22	0.943	122.99
0.18	370	545	61.37	377.02	74.83	170.56	45.62	25.17	0.958	88.80
0.22	370	545	57.15	902.21	85.29	199.51	44.58	14.71	1.124	78.09
0.26	370	545	52.00	421.00	75.14	144.26	50.22	24.86	0.997	75.02

Table S7. Summary of PL lifetimes and pre-exponential factors of $\mathbf{Dy_{1.2}Tb_{3z}Eu_{0.03}Gd_{1.77-3z}W_{28}}$ (*z* = 0.00, 0.10, 0.20, 0.30, 0.40) by monitoring the emission at 572 nm ($^4F_{9/2} \rightarrow {}^6H_{13/2}$) and under the excitation at 389 nm ($^6H_{15/2} \rightarrow {}^6I_{13/2}$).

z	λ_{ex} (nm)	λ_{em} (nm)	τ_1 (μs)	A_1	Percentage (%)	τ_2 (μs)	A_2	Percentage (%)	χ^2	τ^*
0.00	389	572	16.46	985.66	100.00					
0.10	389	572	14.53	848.23	100.00					
0.20	389	572	5.31	586.57	29.17	15.69	482.12	70.83	0.923	12.66
0.30	389	572	4.87	846.56	51.40	14.66	265.78	48.60	0.943	9.63
0.40	389	572	4.05	878.38	60.34	13.36	175.08	39.66	0.928	7.74

Table S8. Summary of PL lifetimes and pre-exponential factors of $\mathbf{Dy_{1.2}Tb_{3z}Eu_{0.03}Gd_{1.77-3z}W_{28}}$ (*z* = 0.00, 0.10, 0.20, 0.30, 0.40) by monitoring the emission at 613 nm ($^5D_0 \rightarrow {}^7F_2$) and under the excitation at 389 nm ($^6H_{15/2} \rightarrow {}^6I_{13/2}$).

z	λ_{ex} (nm)	λ_{em} (nm)	τ_1 (μs)	A_1	Percentage (%)	τ_2 (μs)	A_2	Percentage (%)	χ^2	τ^*
0.00	389	613	68.08	677.45	55.07	198.92	189.15	44.93	0.916	126.85
0.10	389	613	99.97	641.92	52.65	394.91	146.14	47.35	0.998	239.62
0.20	389	613	104.47	276.77	34.89	530.70	101.66	65.11	1.053	382.19
0.30	389	613	155.95	627.77	31.32	801.47	267.83	68.68	0.916	599.28
0.40	389	613	185.89	443.40	19.91	852.59	388.85	80.09	1.032	719.84

Table S9. Comparison of optical parameters for $\mathbf{Dy_{1.2}Tb_{0.3}Eu_{0.03}Gd_{1.47}W_{28}}$ under different excitation wavelengths.

Excitation (nm)	x	y	Dominant wavelength (nm)	CCT (k)	Color purity (%)

360	0.24564	0.33186	491	10913	29.96
361	0.23880	0.32150	490	12060	32.79
362	0.24813	0.31808	489	11416	29.94
363	0.26778	0.33616	492	9128	22.10
364	0.28594	0.36353	500	7537	14.62
365	0.30238	0.38865	518	6593	11.27
366	0.31325	0.40355	537	6132	16.05
367	0.31679	0.40722	542	6003	18.09
368	0.31493	0.40398	539	6074	16.57
369	0.30494	0.39349	523	6469	12.12
370	0.28955	0.37653	505	7221	13.36
371	0.26556	0.35058	495	8888	21.86
372	0.23968	0.32276	490	11903	32.44
373	0.22610	0.30745	488	14505	38.19
374	0.22118	0.29231	487	17056	41.18
375	0.22718	0.28582	486	17175	39.77
376	0.23802	0.29050	486	14892	35.73
377	0.25218	0.30044	486	12179	29.94
378	0.26340	0.31635	488	10169	24.91
379	0.27383	0.33644	492	8719	20.07
380	0.27953	0.34477	494	8181	17.71
381	0.28775	0.34965	496	7634	14.67
382	0.29524	0.35115	498	7219	11.86
383	0.29794	0.35235	499	7069	10.89
384	0.29804	0.35019	498	7086	11.03
385	0.30544	0.36116	505	6636	8.56
386	0.31327	0.37679	524	6222	8.80
387	0.31970	0.38967	540	5942	13.37
388	0.32127	0.39707	544	5873	16.06
389	0.32237	0.40236	546	5828	17.96
390	0.32118	0.40307	545	5866	17.85
391	0.31963	0.40069	543	5922	16.72
392	0.31836	0.39987	542	5967	16.30
393	0.31972	0.39477	542	5931	15.04
394	0.35116	0.38456	566	4892	20.67
395	0.38999	0.37394	582	3740	29.31
396	0.39367	0.37040	584	3619	29.34
397	0.35900	0.37240	573	4603	19.50
398	0.32586	0.37338	544	5744	10.09
399	0.31625	0.37137	525	6123	7.73
400	0.31239	0.37092	518	6282	7.65

Table S10. Comparison of optical parameters for $\mathbf{Dy_{1.2}Tb_{0.6}Eu_{0.03}Gd_{1.17}W_{28}}$ under different excitation wavelengths.

Excitation (nm)	x	y	Dominant wavelength (nm)	CCT (k)	Color purity (%)
360	0.23899	0.35029	494	10616	30.86
361	0.23295	0.33967	492	11533	33.88
362	0.23917	0.33805	492	11128	31.76
363	0.25794	0.34603	494	9490	24.62
364	0.27033	0.36481	498	8317	19.86
365	0.28741	0.39758	512	7119	14.65
366	0.30090	0.41790	530	6498	17.93
367	0.30783	0.42469	538	6245	21.18
368	0.30575	0.42238	535	6320	19.85
369	0.29730	0.41212	524	6651	15.93
370	0.27942	0.39530	508	7466	16.49
371	0.25917	0.37616	499	8684	23.21
372	0.23941	0.35298	494	10485	30.90
373	0.22279	0.33193	491	12831	37.76
374	0.21895	0.32852	491	13422	37.11
375	0.22479	0.31910	490	13586	37.68
376	0.23569	0.32244	490	12286	33.82
377	0.25185	0.33130	491	10452	27.84
378	0.26223	0.34326	493	9292	23.70
379	0.26670	0.35867	497	8637	20.87
380	0.27069	0.36804	499	8241	19.41
381	0.28224	0.37619	503	7557	15.59
382	0.29052	0.37568	505	7186	13.08
383	0.29611	0.37637	508	6934	11.43
384	0.29245	0.37112	504	7143	12.55
385	0.29762	0.37631	509	6870	10.93
386	0.30646	0.39044	523	6427	11.50
387	0.31155	0.40582	536	6183	16.37
388	0.31427	0.41796	542	6060	20.73
389	0.31470	0.42314	543	6034	22.31
390	0.31150	0.42159	540	6138	20.97
391	0.31100	0.42086	539	6156	20.50
392	0.31004	0.42030	538	6189	20.11
393	0.30940	0.41660	537	5221	19.04
394	0.33086	0.40552	553	5553	21.31
395	0.39736	0.38790	580	3668	35.69
396	0.41381	0.38155	584	3257	38.87
397	0.36777	0.38762	573	4417	26.80
398	0.32194	0.39409	544	5855	15.31
399	0.31889	0.39333	540	5963	14.24
400	0.31250	0.39099	531	6199	12.31

Table S11. Comparison of optical parameters for $Dy_{1.2}Tb_{0.9}Eu_{0.03}Gd_{0.87}W_{28}$ under different excitation wavelengths.

Excitation (nm)	x	y	Dominant wavelength (nm)	CCT (k)	Color purity (%)
360	0.22808	0.33083	491	12435	35.96
361	0.22308	0.31981	490	13702	38.23
362	0.23358	0.31656	489	12900	35.00
363	0.25553	0.32694	491	10350	26.66
364	0.26530	0.34876	495	8949	21.81
365	0.27860	0.38174	504	7656	16.47
366	0.29294	0.40587	518	6846	14.76
367	0.30117	0.41273	528	6513	16.52
368	0.29854	0.40851	524	6626	15.23
369	0.28487	0.39194	509	7273	14.87
370	0.26402	0.36590	498	8634	21.60
371	0.24160	0.33837	492	10927	30.94
372	0.22054	0.30667	489	15249	40.10
373	0.20984	0.29123	487	19002	44.99
374	0.20871	0.27549	485	22940	46.41
375	0.21644	0.27639	485	21072	43.92
376	0.22819	0.27497	484	19096	40.29
377	0.24751	0.28373	484	14395	33.21
378	0.25735	0.29875	486	11741	28.55
379	0.25562	0.31103	488	11130	27.98
380	0.26104	0.32231	490	10107	35.17
381	0.27348	0.32894	491	8944	20.49
382	0.28312	0.33066	491	8250	17.17
383	0.28608	0.32747	490	8126	16.38
384	0.28563	0.32632	490	8180	16.59
385	0.29111	0.33273	491	7707	14.42
386	0.29705	0.35113	498	7126	11.39
387	0.30235	0.37223	509	6696	9.72
388	0.30405	0.38946	520	6524	11.24
389	0.30301	0.39555	522	6531	12.50
390	0.30024	0.39589	519	6634	12.57
391	0.29731	0.39202	515	6770	12.26
392	0.29570	0.38867	513	6857	12.25
393	0.29541	0.38058	509	6930	11.85
394	0.33704	0.36445	559	5327	10.46
395	0.42029	0.35069	597	2819	31.20
396	0.43316	0.34781	599	2541	34.53
397	0.37024	0.34598	591	4085	14.92
398	0.31254	0.34145	497	6428	6.53
399	0.30759	0.33691	493	8.57	6716

400	0.30190	0.33171	491	7084	10.74

Table S12. Comparison of optical parameters for $Dy_{1.2}Tb_{1.2}Eu_{0.03}Gd_{0.57}W_{28}$ under different excitation wavelengths.

Excitation (nm)	x	y	Dominant wavelength (nm)	CCT (k)	Color purity (%)
360	0.24843	0.36309	496	9587	27.27
361	0.24231	0.34884	494	10443	29.73
362	0.25436	0.35004	494	9601	26.00
363	0.29752	0.35348	499	7078	11.14
364	0.31314	0.37071	519	5252	7.55
365	0.30061	0.40378	524	6577	14.28
366	0.30384	0.42346	534	6378	19.90
367	0.31132	0.43423	542	6111	24.68
368	0.31315	0.43489	543	6055	25.18
369	0.30321	0.41934	532	6415	18.57
370	0.28898	0.40581	515	6994	15.12
371	0.26857	0.38168	502	8123	19.59
372	0.25007	0.36191	496	9522	26.68
373	0.23801	0.34276	493	11000	31.63
374	0.24333	0.32860	491	11260	30.78
375	0.26578	0.32171	489	9755	23.71
376	0.28595	0.31961	488	8314	17.07
377	0.30916	0.32606	488	6727	8.73
378	0.32837	0.34187	517	5678	1.76
379	0.31283	0.36123	511	6307	6.51
380	0.30839	0.37586	516	6422	8.77
381	0.32532	0.38371	546	5752	13.11
382	0.34254	0.38145	562	5159	17.36
383	0.35204	0.37426	569	4831	17.96
384	0.34975	0.37203	568	4898	16.54
385	0.35156	0.37663	568	4854	18.48
386	0.35463	0.38988	567	4803	23.40
387	0.34426	0.41041	560	5155	26.50
388	0.33540	0.42216	556	5419	27.87
389	0.32449	0.42916	550	5731	26.71
390	0.32181	0.43082	548	5807	26.21
391	0.31884	0.43220	547	5892	26.17
392	0.31870	0.43012	546	5900	25.15
393	0.31944	0.42630	546	5884	24.15
394	0.35612	0.40898	565	4820	29.59
395	0.49317	0.37473	594	2017	60.53
396	0.52521	0.36929	597	1765	68.67
397	0.44720	0.38221	589	2654	48.62

398	0.36825	0.39180	572	4424	28.14
399	0.37669	0.38863	575	4182	29.68
400	0.37117	0.38464	574	4307	26.78

Notes and references

1. M. Bösing, I. Loose, H. Pohlmann and B. Krebs, *Chem. Eur. J.,* 1997, **3**, 1232.
2. G. M. Sheldrick, *SADABS: Program for Empirical Absorption Correction of Area Detector Data*; University of Göttingen, Göttingen, Germany, 1996.
3. G. M. Sheldrick, *SHELXL−97, Program for Crystal Structure Refinement*, University of Göttingen, Göttingen, Germany, 1997.
4. G. M. Sheldrick, *SHELXS−97, Program for Crystal Structure Solution*, University of Göttingen, Göttingen, Germany, 1997.
5. Y. H. Chen, L. H. Sun, S. Z. Chang, L. J. Chen and J. W. Zhao, *Inorg. Chem.,* 2018, **57**, 15079.